Thermochimica Acta, 59 (1982) 267–285
Elsevier Scientific Publishing Company, Amsterdam – Printed in The Netherlands

THE THERMODYNAMIC PROPERTIES OF SOLID COBALT–ZINC ALLOYS

H. CÖMERT * and J.N. PRATT

Department of Metallurgy and Materials, University of Birmingham, Birmingham (Gt. Britain)

(Received 4 May 1982)

ABSTRACT

Reversible potentials of galvanic cells of the form:

$Pt/(Co\text{-}Zn)(alloy) + ZnO/ZrO_2 + CaO/O_2(air)/Pt$

have been measured at temperatures in the range 873–1173 K. The results have been used to derive the thermodynamic activities and the partial and integral free energies, enthalpies and entropies of formation of the α(f.c.c.) solid solutions and of the β_1, γ, γ_1, γ_2 and δ intermediate phases. Exothermic heats of formation and negative entropies of formation are observed throughout the system. The enthalpies of formation of the f.c.c. solid solutions are compared with those of similar cobalt-based examples and the apparent influence of electronic factors is discussed. An analysis is attempted of the factors contributing to the entropies of formation of the solid phases and their Debye temperatures are estimated.

INTRODUCTION

Systematic studies of palladium [1–3] and nickel [4–6] in combination with B sub-group elements have yielded considerable insight into the role of various alloying factors in the thermodynamic properties of such alloys. The recent investigations of those of nickel with Zn [5], Ga[4], Ge [4] or Sn [6] have again demonstrated the particular influences of the electronic structure of the transition metal and it appeared desirable to extend studies to other related first long period alloys. The similarity in the physical properties of nickel and cobalt, together with the dearth of thermodynamic data existing for cobalt + B sub-group metal alloys, suggested that investigations of examples of the latter would be of value. Such a study of the thermodynamic properties of the cobalt–zinc system is reported in the present paper.

The cobalt–zinc alloy equilibrium diagram shown in Fig. 1 is largely as assessed by Hansen and Anderko [7], but modified to incorporate the subsequent experimental determination of the cobalt-rich solidus and liqui-

---

* Present address: Department of Metallurgy, University of Strathclyde, Glasgow, Gt. Britain.

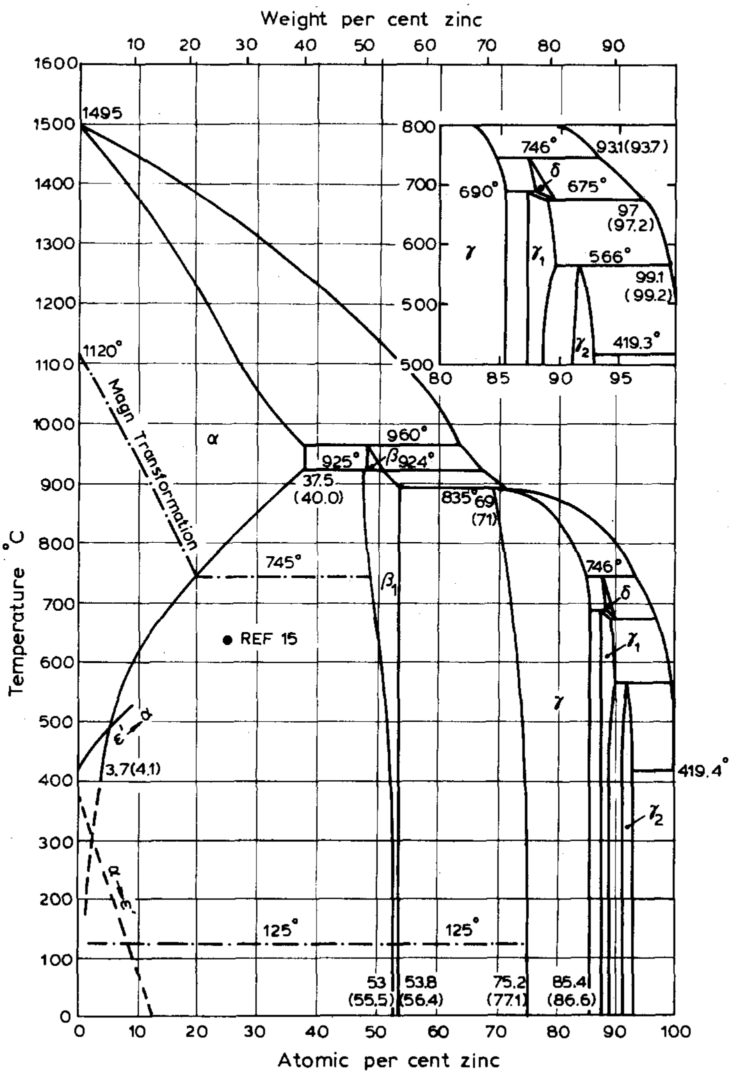

Fig. 1. The cobalt–zinc equilibrium diagram.

dus lines (0–63 atomic % Zn) by Budurov and Wassilew [8]. Solid state phase equilibria are generally well established as a result of extensive thermal, metallographic, X-ray and magnetic studies, particularly by Schramm [9,10]. In addition to the terminal solid solutions, six intermediate phases have been reported. The first of these possesses the β-Mn (A13)-type structure which has led it to be classified as a Hume–Rothery 3/2 electron compound. The structure of the high-temperature β phase has not been established, but a b.c.c. form may be anticipated. A second electron compound (electron : atom ratio 21/13 type) occurs in the form of the γ phase, which exhibits the complex cubic γ-brass ($D8_{1-3}$) structure, while the γ_1 and

γ_2 phases are probably to be regarded as distorted forms of γ. The structure of γ_1 has not been fully determined but γ_2 has a monoclinic unit cell. No structural information has been found for the high-temperature δ phase.

A literature survey revealed four previous partial investigations of the thermodynamic properties of the system. Measurements on solid alloys in the composition range from 0.008 to 86 atomic % zinc and at temperatures between 693 and 883 K were made by Ali and Geiderikh [11], using reversible galvanic cells of the form

$$\mathrm{Zn(liquid)}|(\mathrm{KCl}+\mathrm{LiCl}+\mathrm{ZnCl_2})|\mathrm{Zn}_x\mathrm{Co}_{1-x}\mathrm{(solid)}$$

Their data indicate the system to be characterised by generally negative deviations from ideality. Its integral heats, entropies and free energies of formation show marked compositional asymmetry, with their most negative values occurring near 80 atomic % zinc, that is in the region of the γ phase. A non-monotonic composition dependence of the partial entropies across the homogeneity range of this phase was also noted.

More recently, Budurov et al. [12] have studied the activities of zinc in the Co-rich α-solid-solutions at 1086 and 1300 K using an isopiestic technique, whilst Budurov and Wassilew [13] have made similar measurements of the intermediate β_1 and γ phases between 973 and 1073 K with the aid of the dew-point method. Contrary to the previous observations, both these studies report positive deviations from ideality for the zinc activities in all the phases examined. Great reliance cannot, however, be put on these data since the values reported conflict with the fundamental requirement of invariance of thermodynamic activities across equilibrium two-phase regions.

Finally, very limited studies of liquid cobalt–zinc alloys have been made by Mozeva et al [14], using a modified dew-point technique. Their values for the activities of zinc in dilute alloys (0–2.5 atomic % zinc) at 1813 K again show strong negative deviations from ideality.

It was thus evident that existing thermodynamic knowledge of the system was both limited and contradictory and that further experimental investigation was desirable. New data for most solid phases of the cobalt–zinc system have therefore been obtained by the application of a solid electrolyte galvanic cell technique.

EXPERIMENTAL DETAILS

Alloy preparation

The alloys were prepared from 99.99% pure cobalt (Centre d'Information du Cobalt, Brussells) and 99.995% pure zinc (Imperial Smelting Co., Ltd.), using various procedures to circumvent evaporation losses and other problems caused by the large difference in melting points in the components and the volatility of zinc. In all cases, weighed, chemically cleaned and dried quantities of the pure metals were sealed together in silica capsules which were evacuated and back-filled with argon to a pressure of approximately 0.5 atm. When preparing cobalt-rich α-solid-solution alloys the capsules were heated slowly to 700°C and subsequently, over a period of about 5 days, the temperature was gradually raised to 1150°C. This procedure allowed the absorption of the free zinc without the development of explosive pressures and alloying was then readily completed by induction melting of the encapsulated pre-treated samples. Sequences of gradual heating, but without the need for final induction melting, were similarly successfully employed in preparing all the remaining, more zinc-rich, alloys. In these cases the encapsulated components were first slowly heated to approximately 50°C above the melting point of zinc and, after holding at this point for 24 h, were then further heated in gradual stages over a period of days to about 50°C above the respective alloy liquidus temperature. They were then maintained at these temperatures for up to 4 days, with intermittent shaking to ensure thorough mixing. After melting by either procedure, alloys were quenched to give fine-grained samples and minimise segregation. The resulting ingots, wrapped in tantalum foil and re-sealed in argon-filled silica capsules, were then homogenised for 3 weeks at 850°C (α alloys), 800°C ($\alpha + \beta_1$ and β_1), 700°C ($\beta_1 + \gamma$) or 600°C (γ, $\gamma + \gamma_1$ and γ_1). There was no evidence of alloy contamination, but some minor losses of zinc occurred. Compositions were monitored by carefully weighing after each stage of preparation. Phase structures and sample homogeneity were confirmed by metallographic and Debye–Scherrer X-ray examination of samples taken from several different parts of the ingots. In the case of single-phase alloys, the final compositions were also checked by comparison of the measured lattice parameters with previously established values [15]. With one exception, discussed later, the constitutions of the homogenised alloys were all observed to be consistent with the published phase diagram.

Galvanic cell studies

Measurements were made using an apparatus first established in the authors' laboratory by Bird and co-workers [16]. It is based on the use of a calcia-stabilized zirconia electrolyte (90 mole % ZrO_2 and 10 mole % CaO; Zirconia Corporation of America) and a platinum–air reference electrode, after the manner of Pugliese and Fitterer [17]. The apparatus is shown schematically in Fig. 2; it employs a long zirconia outer tube (L) to enclose the alloy electrode and serve also as the main cell electrolyte; the outer surface of the closed end is platinised (O) to provide the reference electrode. The outer tube is sealed to a water-cooled (A) brass head-plate (B) by an O-ring (G) and locking nut (F). Single alloy/oxide electrodes (P) are contained in a smaller zirconia crucible (N) and enclosed in the main electrolyte tube under a static atmosphere of purified argon admitted via the side tube (D) in the head-plate. The argon was purified by passing over titanium granules at 800°C and a slight positive pressure was maintained inside the apparatus by means of a mercury manometer. The alloy electrode is held in place by two platinum discs and good contact is ensured by a light spring pressure (E) acting through an alumina tube (I). The cell, held horizontally, is located at the mid-point of a Kanthal-wound furnace (M) controlled by a saturable reactor proportional controller (C.N.S. Instruments Ltd.). This controller is activated by a platinum-resistance thermometer (R) and its output to the furnace is rectified by means of a full wave bridge and smoothing circuit; the rectifying bridge consists of four silicon diodes rated at 12 A. By the use of a rectified supply the need for electrical screening inside the furnace was eliminated. The cell is connected by platinium leads (J and K), a glass/metal seal (C) and external co-axial cable to a Farnell Model 3500 Digital Multimeter used to measure the cell potentials. The multimeter is interfaced with a Datel Model DPP7 Printer to monitor potentials automatically over prolonged periods. Cell temperatures are measured by means of a Pt/Pt–13% Rh thermocouple (Q) and digital voltmeter.

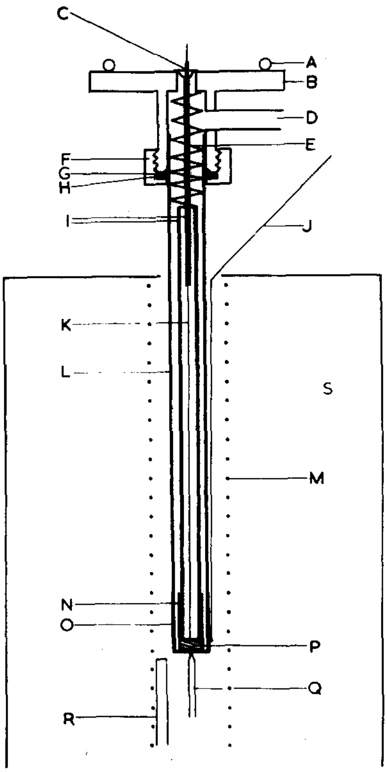

Fig. 2. Solid electrolyte galvanic cell apparatus.

Sieved (200 mesh) powder samples of the alloys, prepared by filing with a diamond file or by crushing in a pestle and mortar, were mixed with ZnO (99.99% purity) in an approximately 7 alloy: 1 oxide weight ratio and tamped down into the small electrolyte crucibles to form the electrodes. After assembly, the sealed system was alternately evacuated and flushed with argon at room temperature before degassing at 200°C overnight. The purified argon atmosphere was then re-established before rapidly heating to the highest temperature to be investigated; the cell potentials were then monitored until stable values were observed. Preliminary investigations of the Co–Zn alloys showed that at very high temperatures zinc evaporation losses were such as to prevent the establishment of stable cells. Such effects were, however, determined by experiment to be negligible below 900°C and, by restricting measurements to this maximum, reliable data were obtained at all the compositions and temperatures reported below. Potentials were measured at approximately 20° intervals chosen randomly in the ranges of interest. Reversibility of the cells was demonstrated by the stability of the measured potentials, their insensitivity to temperature cycling or electrical disturbance and their reproducibility in repeated experiments with new samples.

RESULTS

Fifteen alloys containing from 2.3 to 84 atomic % zinc were investigated over temperature ranges between 873 and 1173 K using cells of the form

$$\mathrm{Pt}/(\mathrm{Co{-}Zn})(\mathrm{alloy}) + \mathrm{ZnO}/\mathrm{ZrO_2} + \mathrm{CaO}/\mathrm{O_2}(\mathrm{air})/\mathrm{Pt}$$

EMF data collected from multiple runs on each alloy composition were treated by least squares analysis to yield the linearly temperature-dependent cell potential equations recorded in Table 1.

For the basic cell reaction

$$\mathrm{Zn}(\mathrm{alloy}) + \tfrac{1}{2}\,\mathrm{O_2}(\mathrm{air}) = \mathrm{ZnO}(\mathrm{solid})$$

the free energy at any temperature T(K)

$$\Delta G = -nFE \tag{1}$$

$$= \Delta G^0_{\mathrm{ZnO}} + RT \ln \frac{a_{\mathrm{ZnO}}}{a_{\mathrm{Zn}} a_{\mathrm{O_2}}^{1/2}} \tag{2}$$

where E is the cell potential (mV), $n = 2$ and $F = 96.483$ J mV^{-1} g eqiv.$^{-1}$. $\Delta G^0_{\mathrm{ZnO}}$ is the standard free energy of formation of ZnO, and a_{Zn} is the activity of Zn in the alloy. Since $a_{\mathrm{ZnO}} = 1$ and $a_{\mathrm{O_2}} = P_{\mathrm{O_2}}(\mathrm{air})$, the above equations are readily re-arranged to yield the partial free energies of solution of Zn, since

$$\Delta \bar{G}_{\mathrm{Zn}} = RT \ln a_{\mathrm{Zn}} = \Delta G^0_{\mathrm{ZnO}} + nFE - \tfrac{1}{2} RT \ln P_{\mathrm{O_2}}(\mathrm{air}) \tag{3}$$

TABLE 1

Temperature dependence of the EMF of the cells $Pt|(Co\text{-}Zn)+ZnO|ZrO_2+CaO|O_{2(air)}|Pt$

x_{Zn}	EMF (mV)	Phase
0.023	$1539.3\pm0.795-(0.5504\pm0.0008)\ T/K$	α
0.031	$1609.5\pm1.305-(0.5655\pm0.0012)\ T/K$	α
0.048	$1648.3\pm1.896-(0.5769\pm0.0018)\ T/K$	α
0.092	$1660.1\pm0.814-(0.5372\pm0.0007)\ T/K$	α
0.436	$1706.3\pm1.976-(0.5194\pm0.0020)\ T/K$	$\alpha+\beta_1$
0.492		
0.515	$1698.5\pm0.613-(0.5059\pm0.0006)\ T/K$	β_1
0.530	$1700.8\pm0.839-(0.5045\pm0.0008)\ T/K$	β_1
0.599	$1680.3\pm1.975-(0.4797\pm0.0020)\ T/K$	$\beta_1+\gamma$
0.644		
0.697		
0.763	$1717.0\pm0.552-(0.5059\pm0.0006)\ T/K$	γ
0.778	$1716.5\pm0.693-(0.4993\pm0.0007)\ T/K$	γ
0.799	$1703.6\pm0.112-(0.4808\pm0.0001)\ T/K$	γ
0.840	$1674.6\pm0.919-(0.4416\pm0.0010)\ T/K$	γ

Required values for ΔG^0_{ZnO} were calculated from the relation

$$\Delta G^0_{ZnO}(\text{J mole}^{-1}) = -353569 + 106.361T \qquad (4)$$

This assessment of the standard free energies of formation of ZnO was itself obtained by combining the free energies of the reaction $Zn(l)+NiO(s)=ZnO(s)+Ni(s)$, as reported by Wilder [18], with measurements of the standard free energy of formation of NiO made in the present studies. The values obtained for NiO $[\Delta G^0(\text{J mole}^{-1})=-232542+83.517T]$ are in excellent agreement with the many previous studies and provide confirmation of the satisfactory operation of the apparatus. An oxygen partial pressure of 0.2095 atm was assumed throughout for the air reference electrode; the effect of variations of atmospheric pressure on the oxygen potential was found to be negligible.

Using the above relationships and cell potentials derived from Table 1, activities and partial free energies of solution of Zn at 1023 K were calculated. The corresponding quantities for the cobalt component were then obtained by integration of the Gibbs–Duhem relation and the integral free energies of formation of the alloys were yielded by the normal summation of the partials. The resulting activities are plotted in Fig. 3, whilst smoothed values of all the quantities are assembled in Table 2. Similar treatment was made of data for 973 and 923 K in order to obtain information for the δ and

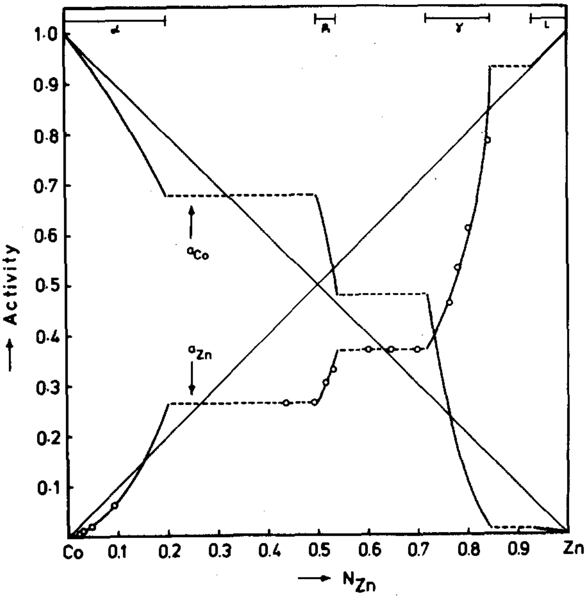

Fig. 3. Activities of cobalt and zinc at 1023 K. [reference states: Co (f.c.c.) and Zn (liq)]. O, Experimental points

γ_1 phases; the corresponding results for these temperatures are presented in Figs. 4 and 5 and Tables 3 and 4. Partial entropies of solution and integral entropies of formation were derived by analogous procedures starting from

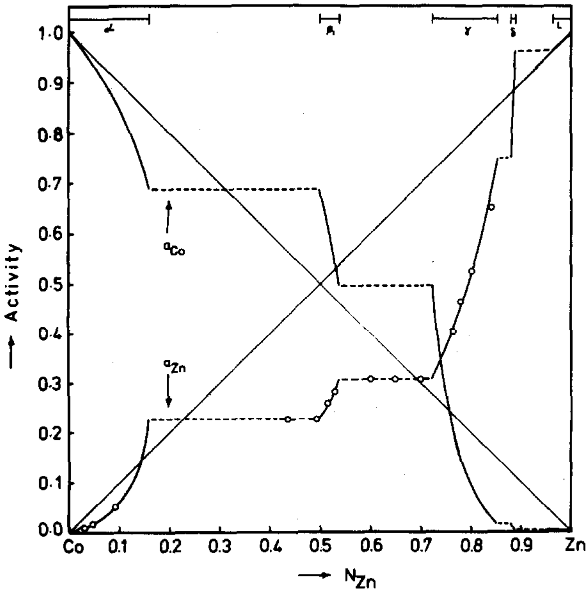

Fig. 4. Activities of cobalt and zinc at 973 K. [reference states: Co (f.c.c.) and Zn (liq)]. O, Experimental points.

TABLE 2

Activities, partial free energies of solution and integral free energies of formation of Co–Zn alloys at 1023 K [reference states: Co(f.c.c.) and Zn(liq.)]

x_{Zn}	a_{Zn}	a_{Co}	$\Delta\bar{G}_{Zn}$ (J g-atom^{-1})	$\Delta\bar{G}_{Co}$ (J g-atom^{-1})	ΔG (J g-atom^{-1})	Phase
0.05	0.024	0.933	−31900	−590	−2160	α
0.10	0.070	0.855	−22620	−1330	−3460	α
0.15	0.142	0.771	−16600	−2210	−4370	α
0.200–0.4975	0.264	0.677	−11330	−3320		$\alpha+\beta_1$
0.51	0.287	0.627	−10620	−3970	−7360	β_1
0.53	0.337	0.528	−9250	−5430	−7450	β_1
0.538–0.7175	0.368	0.477	−8510	−6290		$\beta_1+\gamma$
0.74	0.411	0.355	−7560	−8810	−7890	γ
0.76	0.459	0.256	−6620	−11590	−7810	γ
0.78	0.516	0.172	−5630	−14970	−7680	γ
0.80	0.585	0.107	−4560	−19010	−7450	γ
0.82	0.677	0.058	−3320	−24220	−7080	γ
0.84	0.820	0.022	−1690	−32460	−6610	γ
0.846–0.930	0.930[a]	0.011	−620	−38200		γ+Liq.
0.95	0.950[a]	0.008	−440	−41060	−2570	Liquid
0.98	0.980[a]	0.003	−170	−48860	−1140	Liquid

[a] Extrapolated.

TABLE 3

Activities, partial free energies of solution and integral free energies of formation of Co–Zn alloys at 973 K [Reference states: Co (f.c.c.) and Zn(liq)]

x_{Zn}	a_{Zn}	a_{Co}	$\Delta\bar{G}_{Zn}$ (J g-atom^{-1})	$\Delta\bar{G}_{Co}$ (J g-atom^{-1})	ΔG (J g-atom^{-1})	Phase
0.05	0.017	0.933	−32960	−560	−2180	α
0.10	0.059	0.846	−22890	−1350	−3500	α
0.15	0.168	0.728	−14430	−2570	−4350	α
0.160–0.499	0.228	0.689	−11960	−3010		$\alpha+\beta_1$
0.51	0.247	0.635	−11310	−3670	−7570	β_1
0.53	0.286	0.539	−10130	−5000	−7720	β_1
0.538–0.723	0.308	0.496	−9530	−5670		$\beta_1+\gamma$
0.74	0.351	0.347	−8470	−8560	−8490	γ
0.76	0.400	0.233	−7410	−11780	−8460	γ
0.78	0.456	0.151	−6350	−15290	−8320	γ
0.80	0.520	0.092	−5290	−19300	−8090	γ
0.82	0.590	0.054	−4270	−23610	−7750	γ
0.84	0.680	0.027	−3120	−29220	−7300	γ
0.853–0.880	0.750 [a]	0.015	−2330	−33810		$\gamma+\delta$
0.885	0.890 [a]	0.005	−940	−42090	−5670	δ
0.888–0.964	0.964 [a]	0.003	−300	−46730		δ +liquid
0.98	0.98 [a]	0.002	−160	−51480	−1190	Liquid

[a] Extrapolated.

TABLE 4

Activities, partial free energies of solution and integral free energies of formation of Co–Zn alloys at 923 K [reference states: Co(f.c.c.) and Zn(liq)]

x_{Zn}	a_{Zn}	a_{Co}	$\Delta\bar{G}_{Zn}$ (J g-atom^{-1})	$\Delta\bar{G}_{Co}$ (J g-atom^{-1})	ΔG (J g-atom^{-1})	Phase
0.05	0.012	0.939	−34270	−480	−2170	α
0.10	0.052	0.827	−22690	−1460	−3580	α
0.1225–0.500	0.194	0.702	−12580	−2720		$\alpha+\beta_1$
0.51	0.211	0.644	−11940	−3380	−7750	β_1
0.53	0.242	0.555	−10890	−4520	−7900	β_1
0.538–0.730	0.253	0.527	−10550	−4920		$\beta_1+\gamma$
0.74	0.282	0.393	−9710	−7170	−9050	γ
0.76	0.336	0.227	−8370	−11380	−9090	γ
0.78	0.391	0.136	−7210	−15310	−8990	γ
0.80	0.446	0.087	−6200	−18740	−8710	γ
0.82	0.500	0.053	−5320	−22540	−8420	γ
0.84	0.555	0.031	−4520	−26660	−8060	γ
0.854–0.873	0.590 [a]	0.022	−4050	−29120		$\gamma+\gamma_1$
0.88	0.728 [a]	0.005	−2440	−40500	−7010	γ_1
0.885	0.825 [a]	0.002	−1480	−47690	−6790	γ_1
0.893–0.980	0.980 [a]	0.0005	−155	−58330		γ_1 + liquid

[a] Extrapolated.

TABLE 5

Partial and integral entropies and heats of formation of solid Co–Zn alloys [reference states: Co(f.c.c.) and Zn(liq)]

x_{Zn}	$\Delta\bar{S}_{Zn}$ (J K^{-1} g-atom^{-1})	$\Delta\bar{S}_{Co}$ (J K^{-1} g-atom^{-1})	ΔS (J K^{-1} g-atom^{-1})	$\Delta\bar{H}_{Zn}$ (J g-atom^{-1})	$\Delta\bar{H}_{Co}$ (J g-atom^{-1})	ΔH (J g-atom^{-1})	Phase
0.05	−4.44	+0.03	−0.19	−36440	−550	−2340	α
0.10	−7.76	+0.30	−0.51	−30560	−1020	−3970	α
0.15	−10.36	+0.67	−0.98	−27190	−1520	−5370	α
0.51	−15.03	+3.61	−5.90	−25990	−280	−13390	β_1
0.53	−15.47	+4.09	−6.28	−25080	−1250	−13880	β_1
0.74	−16.54	−0.21	−12.29	−24480	−9030	−20460	γ
0.76	−15.15	−4.32	−12.55	−22120	−16010	−20650	γ
0.78	−16.80	+0.85	−12.92	−22820	−14110	−20900	γ
0.80	−20.15	+13.48	−13.42	−25180	−5220	−21190	γ
0.82	−23.37	+27.21	−14.27	−27230	+3620	−21680	γ
0.84	−27.72	+48.65	−15.50	−30040	+17310	−22460	γ
0.88						−16900[a]	γ_1
0.92						−11250[a]	γ_2

[a] Interpolated.

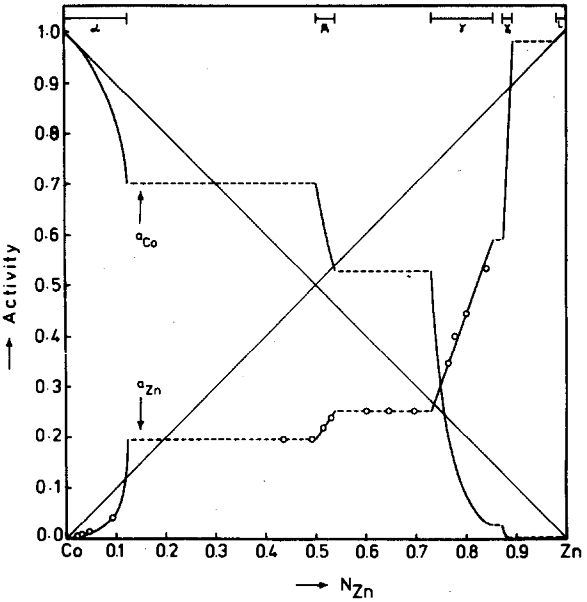

Fig. 5. Activities of cobalt and zinc at 923 K. [reference states: Co (f.c.c.) and Zn (liq)]. O, Experimental points.

the temperature coefficients of Table 1 and eqn. (4). Finally, partial and integral heats of formation were obtained from the free energy and entropy data by means of the Gibbs–Helmholtz relation. The various entropy and enthalpy values are given in Table 5.

All thermodynamic properties are expressed relative to solid cobalt and liquid zinc as standard states.

DISCUSSION

The cell EMF values obtained were consistent with the reported diagram except for the 49.2 atomic % Zn alloy for which the high-temperature behaviour 873–1173 K remained characteristic of the $(\alpha + \beta_1)$ phase field. Metallographic examination of a quenched sample confirmed this two-phase equilibrium and it thus appears that the Co-rich boundary of the β_1 phase rises more vertically than previously reported. Thus, except for the required adjustments in this region, the thermodynamic properties have been evaluated in a manner to accord with the phase boundaries shown in Fig. 1.

The present study demonstrates that the system is generally characterised by negative deviations from ideality. It provides clear confirmation of the behaviour reported by Ali and Geiderikh [11] and contradicts the positive deviations suggested by the work of Budurov et al. [12,13]. Asymmetry of the thermodynamic properties with respect to composition is evident from Fig. 6, where the present results for integral enthalpies and entropies are compared with those of Ali and Geiderikh. Enthalpies of formation yielded by the present investigation are slightly more exothermic than previously reported, but the agreement (±10%) is very satisfactory remembering that each involves second law treatments and Gibbs–Duhem integration. Theoretical values, estimated using the Miedema model [19], are also indicated in Fig. 6. The agreement between experimental and model values is less good than might be expected, but it is perhaps noteworthy that the pattern of discrepancies is similar to that recently observed in the case of Ni–Zn alloys [5].

It is instructive to compare the present results with those for the latter system. The heats of formation of the α-solid-solutions and of the equiatomic intermediate phase are slightly smaller for the Co–Zn examples, but the γ-brass structure phases in the systems exhibit more similar values. However, while this corresponds to the most exothermic point in the Co–Zn system, it is noted that the maximum value in the Ni alloys occurs with the

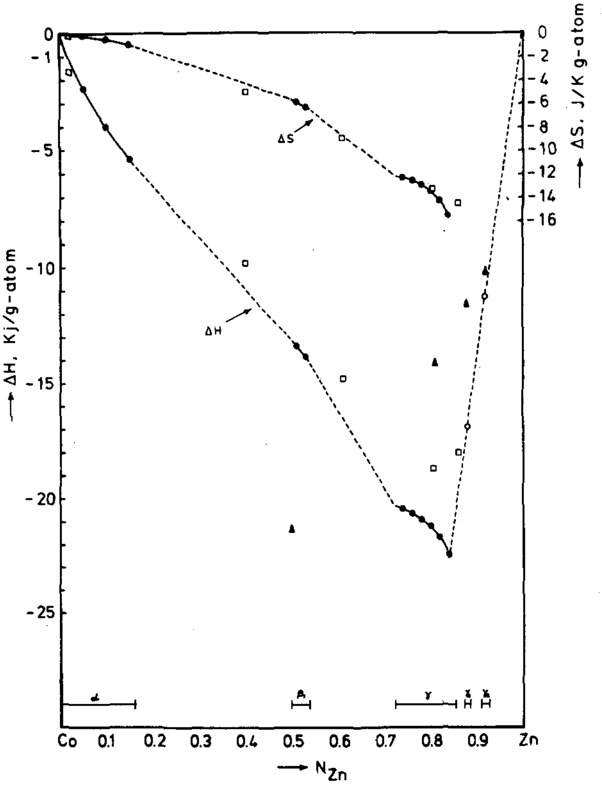

Fig. 6. Integral enthalpies and entropies of formation of solid cobalt–zinc alloys. [reference states: Co (f.c.c.) and Zn (liq)]. ○, Interpolated (present work); ●, present work; □, ref. 30; ▲, calculated (Miedema model).

β_1 phase, i.e., at lower Zn contents. If inter-component electron transfer into the transition metal d-states is assumed to play a significant role in the bonding of the intermediate phases, then the displacement of the maximum enthalpy to the γ phase in the Co–Zn system may be associated with the corresponding shift to higher Zn contents of the point at which d-states are completely filled. The magnetic properties [10,20], suggest that this process is essentially complete in the β_1(Ni–Zn) phase, but may constitute a still increasing effect on passing from the strongly ferromagnetic β_1(Co–Zn) to the weakly magnetic γ(Co–Zn) phase.

The enthalpies of formation of the Co–Zn α-solid-solutions also suggest significant electronic contributions and they may be compared with those for the Co–Ga [21] and Co–Ge [22] solid solutions for which similar data are available. For this purpose, following the analysis suggested by Predel and Stein [23], the heat of formation may be divided into three terms

$$\Delta H = \Delta H_{\mathrm{B}} + \Delta H_{\mathrm{V}} + \Delta H_{\mathrm{U}}$$

where ΔH_{B} is the bonding (electronic) contribution, ΔH_{V} is the atomic misfit strain term and ΔH_{U} is the enthalpy of transformation of the solute from its elemental (reference) structure to that of the solid solution. An estimate of the strain term may be based on Heumann's model [24], according to which

$$\Delta H_V = 0.4\left[T_{\mathrm{A}}\frac{\beta_{\mathrm{A}}}{K_{\mathrm{A}}}(V_{\mathrm{B}} - V_{\mathrm{A}})\, x_{\mathrm{A}}^2 x_{\mathrm{B}} + T_{\mathrm{B}}\frac{\beta_{\mathrm{B}}}{K_{\mathrm{B}}}(V_{\mathrm{B}} - V_{\mathrm{A}}) x_{\mathrm{A}} x_{\mathrm{B}}^2\right]$$

where T is the melting point (°K) of the element, β is its volume coefficient of thermal expansion, K is its isothermal compressibility, V is its molar volume in f.c.c. form, and x is its atom fraction. In the above expression, A denotes Co while B is Zn, Ga or Ge. Values of β and K were taken from Mott and Jones [25] while f.c.c. molar volumes were calculated using C.N.12 radii of the elements from the compilation of Teatum et al. [26]. Values used for the heats of transformation to the f.c.c. lattice were: Zn = 1840 J mole^{-1} (Kaufman and Bernstein [27]), Ga = 8370 J mole^{-1} (Predel and Stein [23]) and Ge = 24000 J mole^{-1} (Miedema [19]). After allowing for strain and transformation enthalpies, the resultant bonding contributions in the three systems are as illustrated in Fig. 7. It is noted that the relative values for the Co–Zn and Co–Ga solutions are approximately proportional to the ratio of the normal valencies (2:3) of the solute elements while the data for the Group IVB element (Ge) fall in an anomalous intermediate position. This may suggest that while Zn and Ga act that their full valencies in inducing transition metal d-band filling, Ge is incompletely ionised. This seems to parallel similar behaviour of the binary solutions of Al and Si in Co where saturation magnetisation measurements [28] suggest that Al acts as trivalent while the Group IVB element (Si) again exhibits less than its maximum valency.

Integral entropies of formation of the α, β_1 and γ phases are well

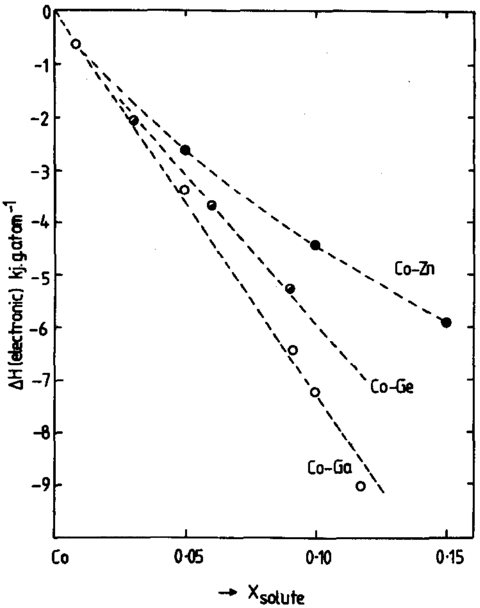

Fig. 7. "Bonding" enthalpies of formation of Co–Zn, Co–Ga and Co–Ge f.c.c. solid solutions.

established by the good agreement between present values and those of Ali and Geiderikh [11]. Third law calculation of the entropies is not possible in the absence of heat capacity data but, instead, an estimate of configurational, electronic and magnetic contributions and of the approximate Debye temperatures of the phases has been attempted by considering available structural and magnetic information. The analysis has been made at the arbitrarily chosen temperature of 1000 K, the total entropies of the phases at this temperature being first derived by combining present entropies of formation with the corresponding entropies of the elements given by Hultgren et al. [29].

It is probably most reasonable to assign random mixing values to the configurational entropies of these phases. The α-solid-solutions would certainly be expected to be fully disordered at the temperature of the analysis and this is likely to be true also of the β-Mn (Co–Zn) phase. No detailed structural information is available for the latter, but evidence from other β-Mn isomorphs [15] indicates that, in the absence of a large electrochemical factor, atomic ordering is unlikely in the present example. The possibility that the γ(Co–Zn) phase exhibits some degree of order is raised by Pearson et al's [30] empirical prediction that it is likely to be based on a stoichiometry Co_4Zn_{22} with Co atoms occupying a single sublattice. A second, non-random, estimate of configurational entropies for this phase was therefore made assuming occupation of this sublattice remains complete while the balance of

Co and Zn atoms are randomly distributed on all other lattice sites.

Electronic entropies have been calculated from the relation $S_{\mathrm{elec}} = \int_0^T \gamma_0 \, \mathrm{d}T$, using electronic specific heat coefficients which are independent of temperature. For the α-solid-solutions, γ_0 values have been obtained by reference to the electronic specific heats of Co–Ni alloys measured by Walling and Bunn [31]. Assuming an unchanged density of states curve, values for the Co–Zn solutions have been estimated from these by interpolation at the corresponding $(s + d)$ electron concentrations. Values for the β_1 examples were calculated using the free electron approximation, so that $\gamma_0 = 9.62 \times 10^{-5} \, (V_A/n)^{2/3}$ J K^{-2} mole elec^{-1}, where V_A is the atomic volume and n is the number of free electrons per atom. Atomic volumes were calculated from the lattice parameters reported by Schramm [9]. Effective valencies of 1 for Co and 2 for Zn must be assumed in this phase since its structure shows it to be a typical 3/2 β-Mn electron compound. The $D8_{1-3}$ structure of the γ(Co–Zn) phase, however, leads it to be classified as a 21/13 electron compound of the γ-brass family and indicates zero effective valency for the transition metal in this case. Associated with this structure is an almost spherical {330}{411} Brillouin zone with first contact of the Fermi surface occurring at 1.537 electrons/atom [25]. Electronic heat capacities for γ-phase compositions up to this point were therefore again calculated from the free electron approximation, but those for post-contact alloys were derived using a still spherical, but segmented, Fermi surface advancing into the corners of the zone after the manner demonstrated for Cu–Zn γ-brass by Veal and Rayne [32]. The values $(\gamma_0 = 0.4)$ used for the $x_{\mathrm{Zn}} = 0.82$ and 0.85 examples were estimated assuming that Brillouin zone overlap is to be expected at about 1.61 electrons/atom. Atomic volumes were again based on X-ray data of Schramm [9].

Only the β_1 phase may be expected to possess a significant magnetic entropy component at 1000 K. No contribution from this source is present in the α-solid-solutions since, although strongly magnetic, they all remain in the ferromagnetic, fully aligned magnetic spin, condition at this temperature [10]. For the γ alloys any magnetic contributions will be trivial in view of the very weak magnetic properties of this phase [9,20]. On the other hand the β_1 phase is strongly ferromagnetic, with Curie temperatures ranging from 471 to 402 K and exhibiting a moment of approximately 1 μ_B per Co atom throughout its range [20]; magnetic entropies arising from the randomisation of these ferromagnetic spins are therefore given by the equation

$$S_{\mathrm{mag}} = R \ln(2\bar{S} + 1) = x_{\mathrm{Co}} R \ln 2$$

After deducting the above contributions from the total entropies, Debye temperatures have been derived from the remainder by assuming that the vibrational contribution may be described by the Debye entropy function $\{S_D(T) - S_D(0)\}$, whilst the small dilatational component is well approximated by $10^{-4}\{U_D(T) - U_D(0)\}$, the Debye internal energy function. The results of this entropy analysis are given in Table 6. The Debye temperatures obtained for the α phase are lower than that for Co given by low-temperature studies [33], but, when compared with an apparent θ_D for the element derived in the present manner from its high-temperature entropy, there would appear to be a systematic increase in Debye temperature with Zn content of the α phase. The value of approximately 350 K found for the β-Mn phase is greater than that of the CuAu($L1_0$)-structure compound occurring at similar compositions in the Ni–Zn system [5]. It is also observed that the Debye temperatures of the present γ-phase are some 60–70 K higher than those of its Ni–Zn isomorph [5]. This suggests that γ(Co–Zn) is more strongly bonded than γ(Ni–Zn) and this may reflect the greater possibility for inter-component transfer to sub-valency levels which exists for the earlier-group transition metal. Clearly the values obtained for the Debye temperature of the γ phase are strongly affected by the exact configurational state assumed. It is interesting, however, that both sets give some indication of passing through a minimum value. Similar trends can be detected in the Debye temperatures of the Cu–Zn γ-brass [32] and it may be noteworthy that in each case the minimum corresponds closely with the composition at which Brillouin Zone overlap is expected to occur.

TABLE 6

Analysis of the entropies of solid Co–Zn alloys at 1000 K (entropy units = J K^{-1} $mole^{-1}$)

x_{Zn}	$S_{elements}$	S_{alloy}	S_{config}	S_{elec}	S_{mag}	$S_{vib+dil}$	θ(K)
0.05(α)	67.17	66.98	1.65	4.44	0	60.88	361
0.1(α)	68.19	67.82	2.70	4.52	0	60.46	369
0.15(α)	69.21	68.23	3.51	4.65	0	60.07	374
0.51(β_1)	76.54	70.64	5.76	0.60	2.82	61.46	353
0.53(β_1)	76.95	70.67	5.75	0.60	2.71	61.61	351
0.74(γ)	81.23	68.94	4.76 [a]	0.62	0	63.56	324 [a]
0.76(γ)	81.64	69.09	4.58 [a]	0.63	0	63.88	320 [a]
0.78(γ)	82.05	69.13	4.38 [a]	0.57	0	64.18	316 [a]
0.80(γ)	82.45	69.03	4.16 [a]	0.46	0	64.41	313 [a]
0.82(γ)	82.86	68.59	3.92 [a]	0.40	0	64.27	315 [a]
0.84(γ)	83.27	67.77	3.66 [a]	0.40	0	63.71	322 [a]
0.74(γ)	81.23	68.94	2.66 [b]	0.62	0	65.66	297 [b]
0.76(γ)	81.64	69.09	2.32 [b]	0.63	0	66.14	291 [b]
0.78(γ)	82.05	69.13	1.93 [b]	0.57	0	66.63	285 [b]
0.80(γ)	82.45	69.03	1.49 [b]	0.46	0	67.08	279 [b]
0.82(γ)	82.86	68.59	0.97 [b]	0.40	0	67.22	278 [b]
0.84(γ)	83.27	67.77	0.30 [b]	0.40	0	67.07	279 [b]

[a] Random model.

[b] Ordered model.

REFERENCES

1 A.W. Bryant, W.G. Bugden and J.N. Pratt, Acta Metall., 18 (1970) 101.
2 J.B. Darby, K.M. Myles and J.N. Pratt, Acta Metall., 19 (1971) 7.
3 J.M. Bird, A.W. Bryant and J.N. Pratt, J. Chem. Thermodyn., 7 (1975) 577.
4 S. Martosudirjo and J.N. Pratt, Thermochim. Acta, 17 (1976) 183.
5 N. Ahmad and J.N. Pratt, Thermochim. Acta, 45 (1981) 139.
6 N. Ahmad and J.N. Pratt, unpublished work, 1979.
7 M. Hansen and K. Anderko, Constitution of Binary Alloys, McGraw-Hill, New York, 1958.
8 S. Budurov and G. Wassilew, Z. Metallkd., 67 (1976) 170.
9 J. Schramm, Z. Metallkd., 30 (1938) 10, 122, 131, 327.
10 J. Schramm, Z. Metallkd., 33 (1941) 46.
11 S.A. Ali and V.A. Geiderikh, Zh. Fiz. Khim., 45 (1971) 1248.
12 S. Budurov, G. Wassilew and L.Mandadshieva, Z. Metallkd., 67 (1976) 307.
13 S. Budurov and G. Wassilew, Z. Metallkd., 68 (1977) 795.
14 A. Mozeva, D. Nenov and N. Gidikova, Arch. Eisenhuettenwes., 48 (1977) 533.
15 W.B. Pearson, Lattice Spacings of Metals and Alloys, Pergamon, London, 1967.
16 J.N. Pratt, J.M. Bird and S. Martosudirjo, Final Tech. Rep. U.S.D.A., Contract No. DAJA37-73-C-3034 (1973).
17 L.A. Pugliese and G.R. Fitterer, Metall. Trans., 1 (1970) 1997.
18 T.C. Wilder, Trans. Metall. Soc. AIME, 245 (1969) 1370.
19 A.R. Miedema, J. Less-Common Met., 46 (1976) 67.
20 A.J.P. Meyer and P. Taglang, C.R., 232 (1951) 1914.
21 I. Katayama, N. Kemori and Z. Kozuka, Trans. Jpn., Inst. Met., 16 (1975) 423.
22 B. Predel and W. Vogelbein, Thermochim. Acta, 30 (1979) 201.
23 B. Predel and D.W. Stein, Acta Metall., 20 (1972) 515.
24 T. Heumann, Z. Elektrochem., 57 (1953) 724.
25 N.F. Mott and H. Jones, The Theory of the Properties of Metals and Alloys, Oxford University Press, London, 1936.
26 E. Teatum, K. Gschneidner and J. Waber, Los Alamos Scientific Lab. Report LA-2345 (1960).
27 L. Kaufman and H. Bernstein, Computer Calculation of Phase Diagrams, Academic Press, New York, 1970.
28 D. Parsons, W. Sucksmith and J.E. Thompson, Philos. Mag., 3 (1958) 1174.
29 R. Hultgren, P.D. Desai, D.T. Hawkins, M. Gleiser and K.K. Kelley, Selected Values of the Thermodynamic Properties of the Elements and Alloys, American Society for Metals, Metals Park, Ohio, 1973.
30 W.B. Pearson, J.K. Brandon and R.Y. Brizard, Z. Kristallogr., 143 (1976) 377.
31 J.C. Walling and P.B. Bunn, Proc. Phys. Soc., 74 (1959) 417.
32 B.W. Veal and J.A. Rayne, Phys. Rev., 132 (1963) 1617.
33 E.S.R. Gopal, Specific Heats at Low Temperatures, Heywood, London, 1966.